Soldering Si3N4 to Invar42 by a localized heating process

Received: 23 July 2025 | Revised: 24 October 2025 | Accepted: 28 October 2025

DOI: 10.1111/ijac.70118

International Journal of Applied Ceramic Technology

RESEARCH ARTICLE

# Soldering Si3N4 to Invar42 by a localized heating process

**Stefano De La Pierre**[1] | **Alessandro Benelli**[1] | **Monica Ferraris**[1] | **Daniela Di Martino**[2] | **Fabio Vivenzio**[2] | **Rebecca Napolitano**[2]

[1]Department of Applied Science and Technology and J-Tech@PoliTO, Politecnico di Torino, Torino, Italy

[2]MBDA—Fusaro, Napoli, Italy

**Correspondence**
Stefano De La Pierre, Department of Applied Science and Technology and J-Tech@PoliTO, Politecnico di Torino, Corso Duca degli Abruzzi 24, 10129 Torino, Italy.
Email: stefano.delapierre@polito.it

**Abstract**

This study investigates the soldering process for joining silicon nitride ($Si_3N_4$), a commonly used ceramic, to Invar42, a low thermal expansion alloy. The focus lies on analyzing interfacial reactions and evaluating the bonding performance of the $Si_3N_4$—Invar42 joint. Field emission scanning electron microscopy (FESEM) and energy-dispersive X-ray spectroscopy (EDS) were employed to examine the microstructure, elemental distribution, and chemical composition of the interfacial region. The results underscore the critical role of interfacial reaction layers in the soldering process. Mechanical testing (single lap offset, SLO, lap shear tests) was conducted to assess the bonding strength and mechanical integrity of the soldered joints. Furthermore, the thermal stability and reliability of these joints were evaluated through SLO tests at 300°C. This study contributes to the advancement of a user-friendly, pressureless, localized heating and field-deployable technique for soldering $Si_3N_4$ to Invar42, thereby facilitating the fabrication of advanced engineering systems in industrial environments.

KEYWORDS
invar, silicon nitride, soldering

## 1 | INTRODUCTION

The successful integration of dissimilar materials is of paramount importance in various engineering applications. Joining silicon nitride ($Si_3N_4$), a widely used ceramic material, to Invar42, a low thermal expansion alloy, presents unique challenges due to the stark differences in their material properties.

$Si_3N_4$ is a versatile advanced ceramic widely employed in automotive and aerospace engineering, where components must withstand extreme thermal and mechanical loads—for example, in turbochargers, fuel injectors, and exhaust gaskets. It exhibits a high melting point, excellent electrical and thermal conductivity, acid and wear resistance, and a low thermal expansion coefficient. These characteristics make it suitable for use in high-temperature, high-strength environments.[1] Its potential in structural applications, such as engine and cutting tools, is well established due to its mechanical robustness and thermal stability.

In contrast, Invar42 is a 42% nickel–iron controlled expansion alloy, renowned for its extremely low coefficient of thermal expansion (CTE) at room temperature ($\sim 2 \times 10^{-6}$ $K^{-1}$). However, its CTE increases significantly at elevated temperatures, complicating joint design with ceramics. Despite this, Invar42 is valued for its dimensional stability and has found applications in aerospace, instrumentation, and solar energy systems. Its thermal

conductivity and relatively high melting point further enhance its attractiveness for components subjected to variable thermal loads.

The joining of $Si_3N_4$ to Invar42 has been attempted via conventional methods such as brazing, soldering, and diffusion bonding, often with systematic parameter optimization. However, most studies reveal that substantial challenges remain, primarily due to poor wettability of $Si_3N_4$ and CTE mismatch between the ceramic and the metal.[2] A foundational review by Peteves et al.[3] highlighted the technical limitations of $Si_3N_4$ joint performance in high-temperature environments. Although significant progress has since been made,[4–18] their warning—that much work is still needed for hot-stressed applications—remains partially valid today. Despite various joining attempts with metals (stainless steel, superalloys, Ni-, Mo-based alloys), poor wetting and thermo-mechanical incompatibility continue to impede joint reliability. A comprehensive review by Singh and Asthana[19] explored two decades of $Si_3N_4$-metal joining research using braze interlayers with liquidus temperatures ranging from 750°C–1240°C. Notably, active brazes—incorporating elements like Ti—emerged as critical for achieving wetting and bonding to $Si_3N_4$. Active brazes such as Cu-ABA demonstrated success due to chemical reactivity at the ceramic interface. While stress compensation via pure Cu interlayers has shown promise, it adds complexity and may not fully mitigate thermal mismatch stresses. One of the earliest studies addressing $Si_3N_4$–Invar bonding was conducted by Suganuma et al.,[20] who used an aluminum interlayer above its melting point. The resulting intermetallic layers at the Al–Invar interface offered mechanical strengths of 150–200 MPa. However, the method was limited by crack formation in the intermetallic layers and lacked evidence of thermal stability, which is essential for practical applications. The necessity of precise control over bonding temperature and time further reduces its scalability. More recent efforts by Wang et al.[21] introduced a three-layer brazing structure (AgCuTi+TiN particles/Cu/AgCu), where TiN particles reduced CTE mismatch and a Cu layer accommodated residual stress. This approach achieved a high shear strength (256 MPa) and significant reduction in residual stress, supported by FE modeling. However, the complexity of this layered system may limit its industrial feasibility, especially in cost-sensitive applications.[22] A similar strategy using Cu–Ti filler alloys was proposed in Sun et al.,[18] where Ti served as the reactive element to form TiN and $Ti_5Si_3$ at the interface. However, the decomposition of $Si_3N_4$ and formation of brittle phases may compromise long-term mechanical reliability. To address CTE mismatch, Shirzadi et al.[23] proposed using metallic foams as buffer layers. These structures accommodate stress through their porous architecture and have demonstrated resilience under thermal cycling. Guo et al.[24] applied this strategy with AgCuTi and Ni foam for $Si_3N_4$–Invar joining. Although the foam reacted with the filler, its core structure remained, contributing to a robust bond and shifting fracture modes away from the ceramic. This strategy presents a promising compromise between mechanical strength (180 MPa) and thermal cycling resistance.[25] An alternative to foams is the use of metallic multilayers,[26–28] designed to tailor the interfacial stress response by adjusting the CTE and yield strength gradient. While still under development, multilayer systems hold promise for fine-tuning joint behavior, but the temperatures involved cannot completely avoid stress concentrations. Additionally, the complexity of the multilayer process might be difficult to scale up.

Recent investigations into the joining of silicon nitride ($Si_3N_4$) ceramics to Invar 42 alloys have introduced two distinct approaches: one utilizing a molybdenum (Mo) mesh interlayer, and another incorporating a hybrid Mo mesh and copper (Cu) foil configuration. In Zhao et al.[29] vacuum brazing at 880°C with Ag27.5Cu4.5Ti filler yielded robust metallurgical bonding characterized by the formation of TiN and $Ti_5Si_3$ phases at the ceramic interface. The introduction of a Cu foil interlayer significantly enhanced joint performance, increasing shear strength from 191.7 MPa to 235.5 MPa. This improvement was attributed to the suppression of brittle $Fe_2Ti$ and $Ni_3Ti$ intermetallics at the Invar interface, facilitated by the Cu foil's role in promoting plastic deformation and mitigating residual stresses. Complementary findings from Salvo et al.[30] employing Ag–Cu–In–Ti filler with a Cu foil interlayer corroborated the mechanical benefits of interlayer engineering. The multi-layer configuration disrupted the continuity of deleterious intermetallic phases and redistributed stress concentrations, resulting in an 82% increase in shear strength compared to joints formed with a single-layer filler. Active brazing with intermediate or compliant layers (e.g., Cu or foams or meshes) appears most effective in mitigating thermal mismatch and achieving strong joints. However, the processing complexity, high temperatures, and limited long-term data remain barriers to practical application.

In summary, the literature demonstrates a broad range of approaches for joining $Si_3N_4$ to metals, including Invar42 and joining methods can be broadly compared by considering mechanical performance, processing cost, and scalability: structural adhesives offer the lowest cost and easiest scalability with moderate strength but generally lack thermal stability; high-temperature methods such as active metal brazing and transient liquid phase (TLP) bonding achieve the highest mechanical strengths, frequently exceeding 100 MPa shear strength, due to formation of reactive interfacial phases and strong

metallurgical bonds.[4, 19, 24] These techniques require vacuum or controlled atmospheres, high processing temperatures (often > 800°C), and precise control of interlayer chemistry, which increase equipment costs and limit scalability and localized joining.

It is also noteworthy that most successful joining strategies rely, in some cases, external pressure or surface modification.[31] These requirements may be incompatible with thermally sensitive components or cost-effective manufacturing. In contrast, active solders like S-Bond™ enable low-temperature (≤450°C), flux-free, and localized joining, offering moderate mechanical strength and good hermeticity, while significantly reducing thermal stress and energy consumption.[32] These features make active solders attractive for temperature-sensitive or complex geometries but often require surface modification or interlayers to reach strengths competitive with brazing. Notably, few studies directly address the long-term stability of $Si_3N_4$–Invar joints, and only a handful explore scalable or cost-effective routes. Therefore, further research is required to develop joining techniques that:

- Operate at moderate temperatures to reduce energy input and residual stress
- Maintain high mechanical strength and thermal stability
- Are compatible with industrial-scale processing
- Specifically optimize for the $Si_3N_4$–Invar42 material pairing

As a lower-temperature alternative, soldering has been explored,[32] using tin-based, lead-free solders enriched with Ti. These materials rely on a combination of metallurgical bonding (via intermetallic formation with Cu or Al) and van der Waals "gravity bonding" with oxide-covered surfaces. Soldering avoids thermal degradation and offers plasticity to relieve residual stress. One example, S-Bond™, incorporates active elements that disrupt oxide layers and promote bonding. As soon as the oxide layer is disrupted, the solder volume reacts with the substrate surface, and a strong bond with the joined surface is thus formed.

Mechanical activation is also an option, and it may be realized by:

- scratching and spreading with a metal brush
- vibrations (50 Hz–60 Hz)
- ultrasound with the frequency over 20 kHz, suitable for soldering ceramic and non-metallic materials.

In this way, the necessity of a vacuum, shielding atmosphere or multistep solder deposition is eliminated and localized heating is possible. For the soldering of metals, it is mostly sufficient to activate mechanically by scratching, but in the case of ceramic materials, it might be necessary to employ ultrasonic activation with the frequency over 20 kHz. However, the application of ultrasonic method is sometimes limited: in the case of brittle substrates such as ceramics, the damage of specimen by cracking the surface layers may occur. While attractive for low-temperature applications, the mechanical reliability and thermal endurance of such joints remain underreported, particularly in the case of $Si_3N_4$–Invar assemblies.

The aim of this study was to find a joining technique for components based on $Si_3N_4$ joined to Invar42, with a working temperature of about 300°C, a lap shear strength 35 MPa ÷ 40 MPa, hermeticity and humidity resistant behavior; a pressureless, localized heating joining process potentially adaptable to curved surfaced and suitable to be used in an industrial environment was also preferred. After thorough screening, testing and down-selecting some suitable materials and technologies, the activity was focused on a soldering alloy, S-Bond ® Alloy 400, (S-Bond in the following text).

S-Bond has numerous industrial applications, including solar panel assembly, semiconductor processing, and packaging optical devices. Its transformative potential lies in scenarios requiring *localized heating to join intricate structures*, such as sealing sapphire windows to metal enclosures. S-Bond offers a low-temperature, flux-free, hermetic, ductile and reworkable solution, ideal to join ceramics to steel, Ti, Cu, Al, etc.[32]

## 1.1 | Experimental part

Silicon nitride was produced by MBDA Italia S.p.A., by a patented process[33] and has a CTE of about $3 \times 10^{-6}$ $K^{-1}$ measured between 125°C and 1000°C. Invar42 was supplied by MBDA Italia S.p.A. Both materials have a roughness of about *Ra* 5–7, obtained by paper gritting (#120) and measured by surface stylus profiler (Taylor Hobson ™—Intra Touch™). The selected alloy S-Bond ® Alloy 400, was supplied by S-Bond Technologies, LLC, USA as wires[32]: its composition, as provided on the data sheet, is: Zn 87%–91%, Ag 4%–6%, Al 4%–6% plus Ga and Cr 0.1%–0.3%, and other elements 0%–0.2% (% wt). The thermal coefficient of expansion from room temperature to 300°C is $\sim 32 \times 10^{-6}$°$C^{-1}$.

The pressure less soldering process was initially done on a hotplate in air at about 450°C, then with an electric heather able to melt the S-Bond; process temperatures were measured by an optical pyrometer. S-Bond was applied on both the surfaces to be joined: once molten on both surfaces, the two faying surfaces were overlapped and manually shacked one on the other one to mechanically activate the solder. Some samples were sputtered by Zn,

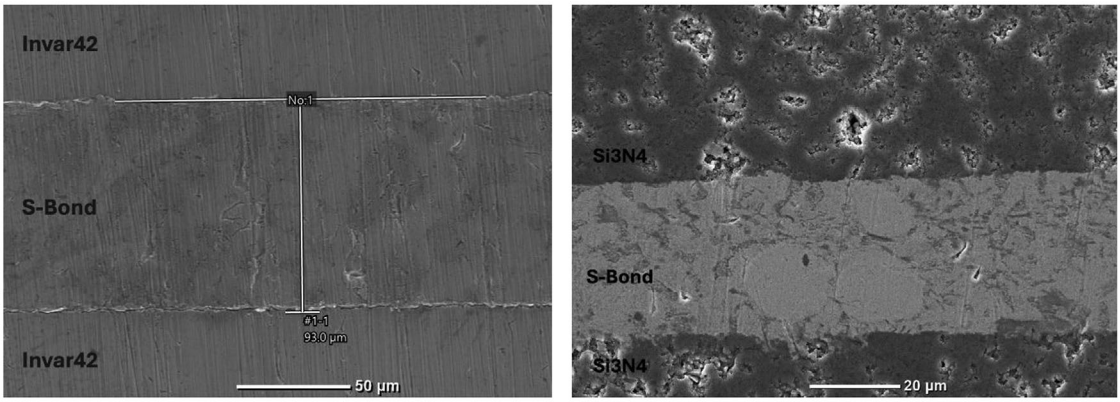


**FIGURE 1** SEM of S-Bond joints, polished cross-sections: Invar42 to Invar42 (A) and $Si_3N_4$ to $Si_3N_4$ (B).

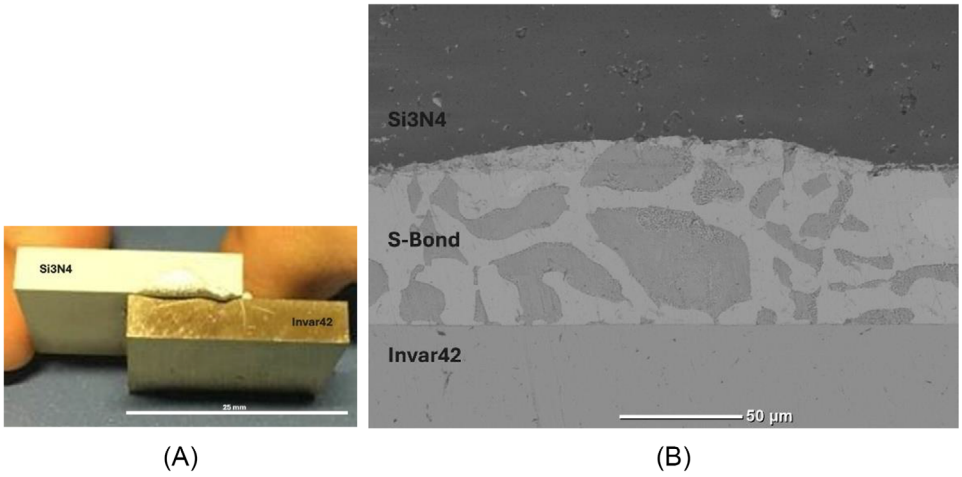


**FIGURE 2** S-Bond joints ($Si_3N_4$ to Invar42, visual inspection) (A); SEM polished cross section of $Si_3N_4$/S-Bond interface (B).

Cr, Ti, or Al before soldering, by using a sputtering system from Kenosistec™ with the following deposition parameters: deposition time 8 h, power supply 250 W (DC) on 3 inches diameter targets, pressure 7.3 dPa, with 25 sccm Argon (Ar) flow, pre-process vacuum $9 \times 10^{-5}$ mbar (9 mPa), substrate rotated at 20 rpm. The distance between cathode and substrate was 14 cm. A metallic (Zn, Cr, Ti, Al) 99.99% pure targets from NanoVision™ were used. The Zn, Cr, Ti, or Al sputtered layer was measured by surface contact stylus profilometry (Taylor Hobson Intra Touch 3D).

Single lap offset (SLO) mechanical tests were performed by Zwick Roell (Z050 THW) on joined samples at room temperature and at 270°C in air: slabs measuring 25 mm × 25 mm × 5 mm were joined with an offset of 12.5 mm and tested in compression according to a method adapted from ASTM D905-08. The crosshead speed was 0.5 mm/min; the lap shear was obtained by dividing the maximum load at fracture by the bonded area.

The cross-sectional morphology of joined samples was characterized by optical microscopy and electronic microscopy using Field Emission Scanning Electron Microscopy (FESEM-ZEISS Supra 40) with an Energy Dispersive Spectroscopy (EDS- SW9100 EDAX) detector. Morphological analysis on fracture surfaces obtained after mechanical tests has been also performed.

## 2 | RESULTS AND DISCUSSION

S-Bond Technologies initially developed in 1996 a Sn–Ag–Ti active solder alloy that was found to bond to most metals, ceramics and composites without the use of Cd. S-Bond is the highest temperature active solder of this family, with a soldering process between 420°C and 430°C: the suggested pressure to be applied is about 16 kPa and the optimum joining material thickness is between 62 and 75 µm.

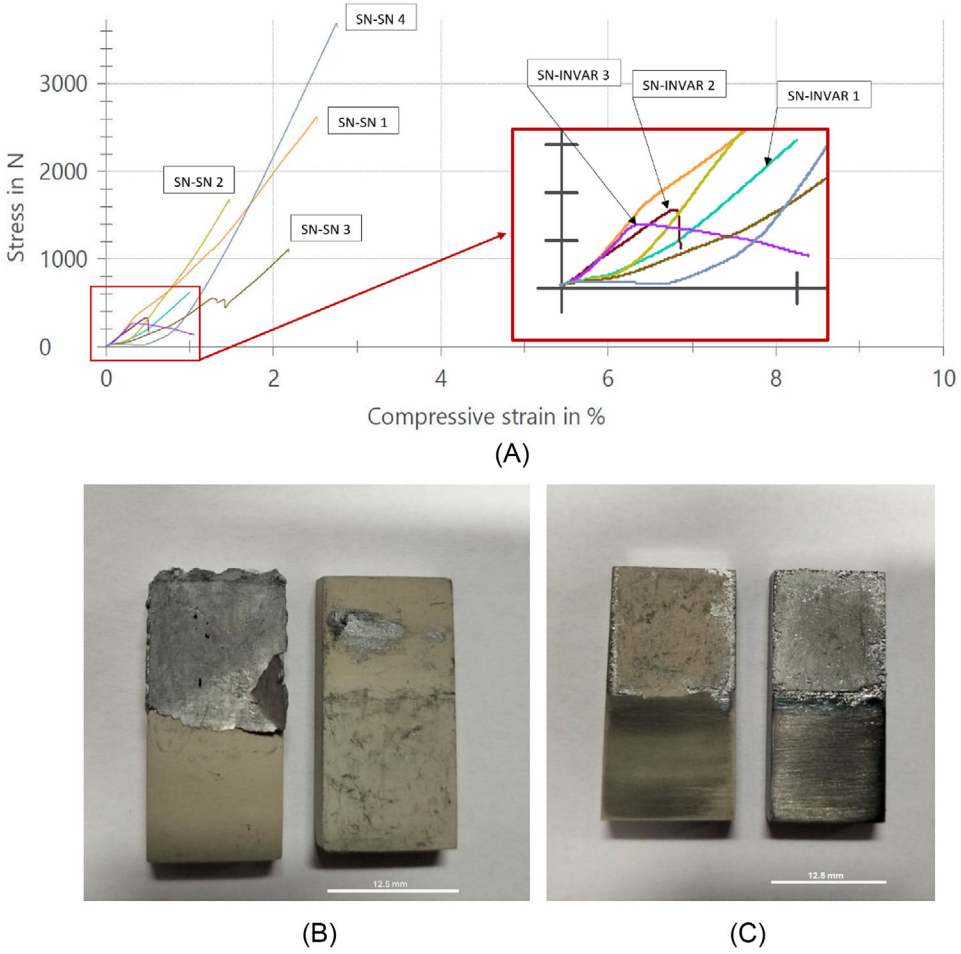


**FIGURE 3** Single Lap Offset (SLO) test in compression on samples joined by S-Bond, room temperature: Si3N4 to Si3N4 and Si3N4 to Invar42 (A) showing higher mechanical strength for Si3N4 to Si3N4 samples (11 ± 4 MPa); fracture surfaces of Si3N4 to Si3N4 (B) and Si3N4 to Invar42 (C) samples (2.7 ± 1.2 MPa) after mechanical test.

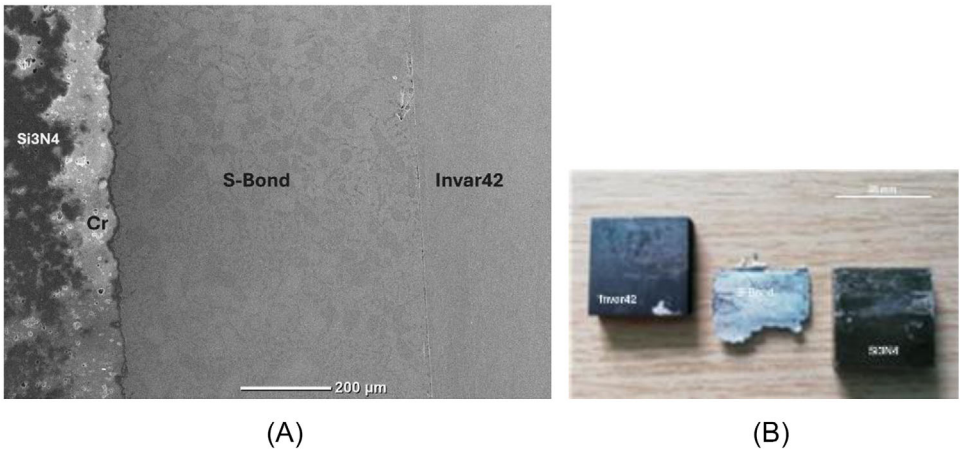


**FIGURE 4** S-Bond joined Cr-sputtered Si3N4 to Invar: SEM cross section (A) and visual inspection of the joint showing complete detachment (B).

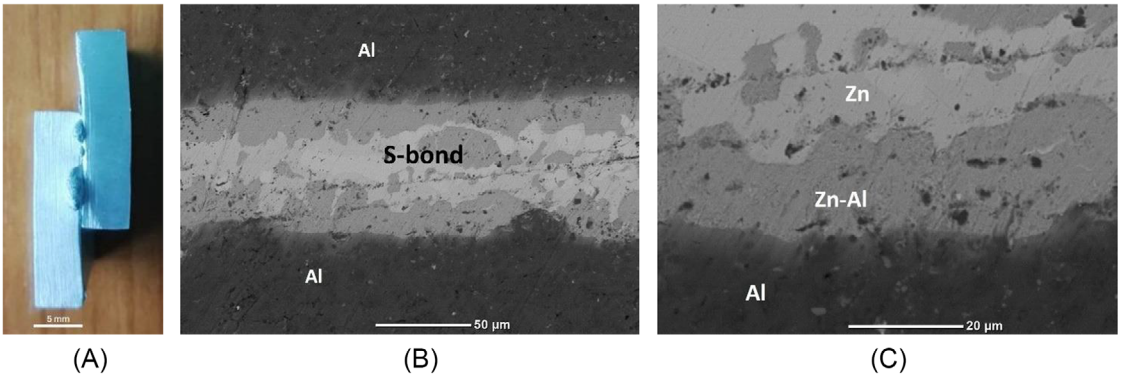


**FIGURE 5** S-Bond joined Aluminum to Aluminum samples after SLO test (about 58 MPa) (A); polished cross section of S-Bond joined Al to Al samples (B) and results of EDS analysis on higher magnification of the interface (C).

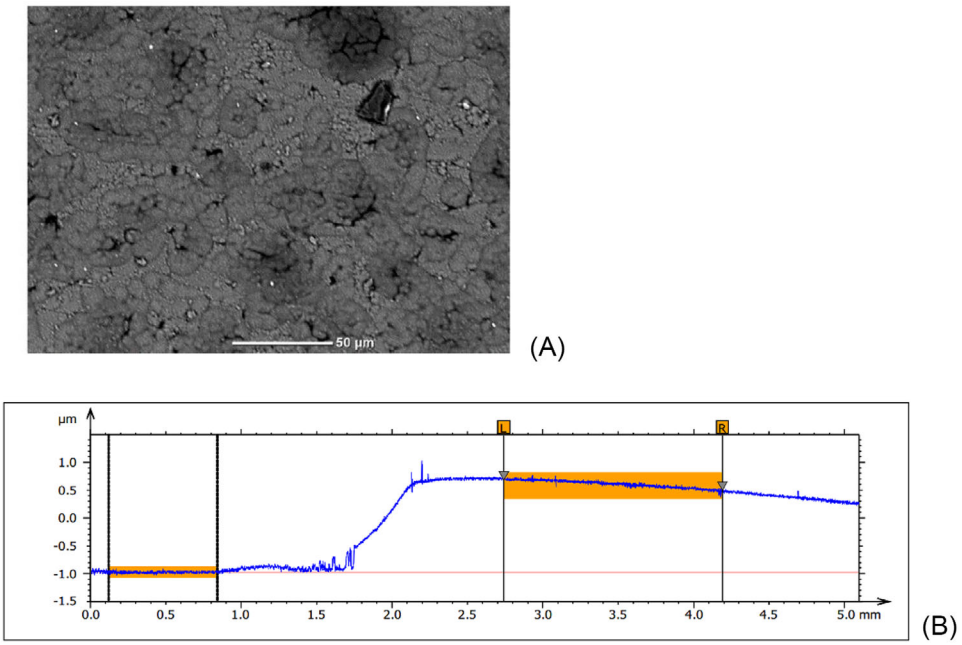


**FIGURE 6** The SEM top view of Al sputtered $Si_3N_4$ (A) with the typical globular morphology of sputtered materials; EDS analyses (not reported) confirmed the presence of Al as the only detected element; the sputtered Al layer thickness was measured by profilometry, and ranged between 1.5 and 2 µm: one example of profilometry is in B.

However, for the discussed application, a pressureless joining method was preferred.

Slabs of about 25 mm × 25 mm × 5 mm joined in a single lap offset configuration with the joining material sandwiched between were prepared, cross sectioned and analyzed by FESEM and compositional analysis.

Figure 1 shows the obtained S-Bond joints: Invar42-to-Invar42 (Figure 1A) and $Si_3N_4$-to-$Si_3N_4$ (Figure 1B); the bond line is continuous and fractureless, demonstrating the suitability of this solder to pressureless join these two materials, by a localized heating source. This solder alloy has a very high thermal expansion coefficient, if compared to that of the two facing materials, but the ductility of the braze helps to reduce stresses in the joint.

The following step was to obtain the $Si_3N_4$-to-Invar42 joint with the same procedure: Figure 2 shows the visual appearance of a S-Bond joined $Si_3N_4$-to-Invar42 (Figure 2A) and a SEM on the polished cross section (Figure 2B).

Single Lap Offset (SLO) tests were done at room temperature on S-Bond joined $Si_3N_4$-to-Invar42 (on 4 samples) and on $Si_3N_4$-to-$Si_3N_4$ (3 samples): results are shown in Figure 3A. A striking difference in mechanical strength was found, with a much higher value for the $Si_3N_4$-to-$Si_3N_4$ samples (11 ± 4 MPa) than for $Si_3N_4$-to-Invar42

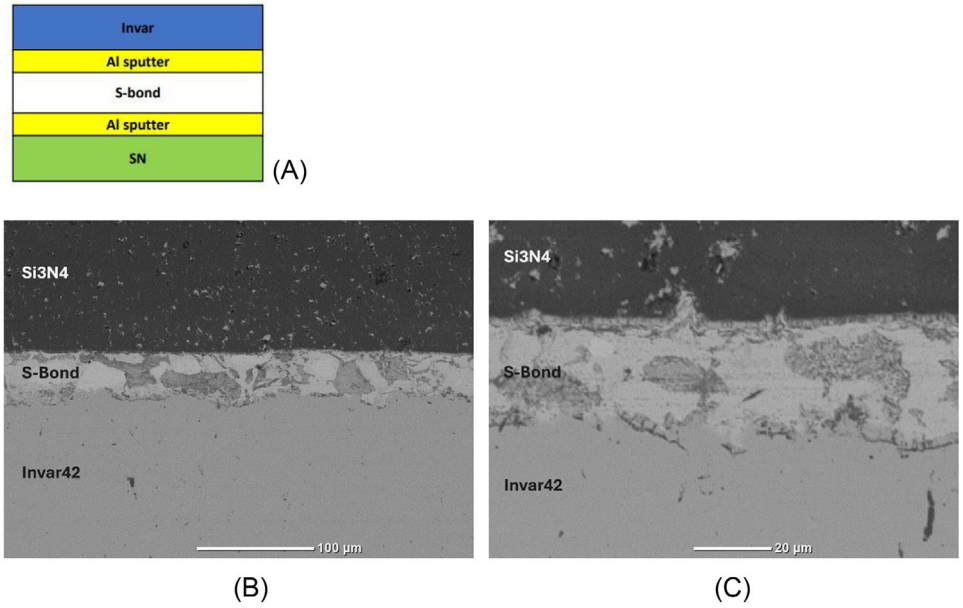


**FIGURE 7** Al-sputtered Si3N4 and Invar42 joined by S-Bond: sketch (drawing not to scale) (A) and SEM polished cross section: a thin interface layer formed between S-Bond and the Al sputtered layers (B, C) on both Si3N4 and Invar. As a comparison, see the absence of such a reaction layer between S-Bond and Invar to Si3N4 joint in Figure 2B.

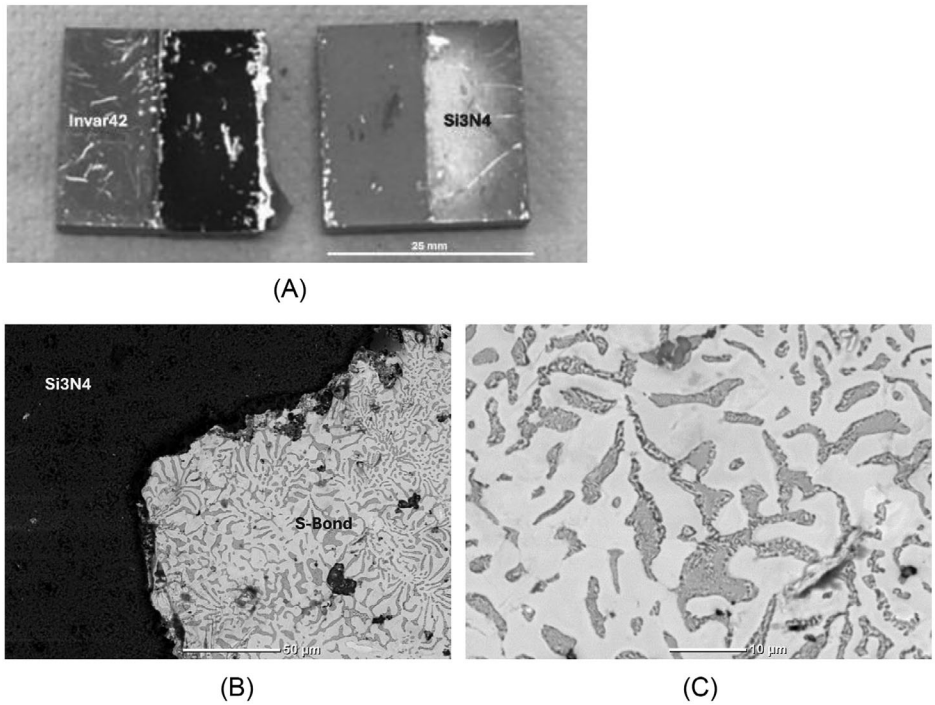


**FIGURE 8** Al-sputtered Si3N4 and Invar42 joined by S-Bond: samples after mechanical test (SLO, 26 ± 7 MPa): the joining material is visible on both sides (A); SEM of the fracture surface (B, C) showing reaction zone between sputtered Al and S-Bond (bi-phasic region with eutectic structure).

ones (2.7 ± 1.2 MPa). The typical fracture surfaces are in Figure 3B and D, showing a partially adhesive failure mode with most of the solder alloy on one side of the fractured specimen. In particular, the failure of $Si_3N_4$-to-Invar42 samples seemed to be due to a weak interface with $Si_3N_4$: most of the soldering alloy is left on the Invar42 (Figure 3C); this is a typical feature observed when there is a weak interface, which fails.

To improve the S-Bond adhesion to $Si_3N_4$, $Si_3N_4$ slabs were sputtered by Zn, Cr, or Ti, then joined to Invar42; all of them showed an improved adhesion, but still not sufficient to give a sound mechanical strength: some joints failed during cutting, with S-Bond bonded only to Invar42 or completely separated from the two substrates. Figure 4 shows, as an example, the results obtained with Cr sputtered $Si_3N_4$: S-Bond did not form any evident reaction layer with Cr sputtered on $Si_3N_4$ and the joined sample failed at about 2 MPa, with the S-Bond completely detached from the two substrates. S-Bond main element is Zn and by observing the Cr-Zn phase diagram (not reported here), it can be seen that 450°C is too low to obtain a liquid phase able to form a reaction layer during the short bonding process. Even though the wettability of S-Bond on Cr is excellent, the absence of interfacial reactions leaves the S-Bond compositionally unchanged and unable to bond the two substrates. A possible reason for such unsatisfactory results is the lack of reactivity between S-Bond and the faying surfaces; however, the data sheet reports a joint strength at room temperature for S-Bond joined Aluminum to Aluminum as ranging between 80 and 110 MPa; in order to verify it, some S-Bond joined Aluminum to Aluminum and steel to steel samples were prepared with the same procedure used before and tested with the same SLO test.

S-Bond joined Aluminum to Aluminum did not break at 58 MPa and the test was stopped at Al plastic deformation. (Figure 5A). On the contrary, S-Bond joined steel to steel (picture not reported) failed while in the testing fixtures; by considering the Fe-Zn phase diagram (not reported), a process temperature of 450°C is too low to obtain a liquid phase assisted reaction between Fe and Zn, able to form a reaction layer during the short bonding process. Also in this case, even though the wettability of S-Bond on steel is excellent, the absence of interfacial reactions leaves the S-Bond compositionally unchanged and unable to bond the two substrates.

The sound interface between S-Bond and Al seems to be the reason for the higher strength of these samples and was thoroughly investigated by SEM and EDS analysis, as reported in Figure 5B and C: it shows a reaction layer of about 20 μm between Al and S-Bond, which contains Zn and Al rich phases, according to the Al-Zn binary phase diagram, presenting liquid phases at 450°C.

According to these results, it was decided to sputter Al on #120 paper gritted $Si_3N_4$ and Invar42 before S-Bond joining.

Figure 6 shows SEM top view of Al sputtered Si3N4 (Figure 6A) with the typical globular morphology of sputtered materials; EDS analyses (Figure 6B) confirmed the presence of Al as the only detected element. The sputtered Al thickness measured by profilometry ranged between 1.5 and 2 μm (Figure 6B).

**TABLE 1** Summary of the SLO (single lap offset shear strength test) results at room temperature and at 270°C.

| S-Bond joined sample | Lap shear (MPa) |
|---|---|
| Al/Al | >58 |
| $Si_3N_4/Si_3N_4$ | 11 ± 4 |
| $Si_3N_4$/Invar42 | 2.7 ± 1.2 |
| Al sputtered $Si_3N_4$/Invar42 (RT) | 26 ± 7 |
| Al sputtered $Si_3N_4$/Invar42 (270°C) | 14 ± 4 |
| Cr sputtered $Si_3N_4$/Invar42 | 2 |

In order to verify if the formation of a reaction layer between S-Bond and the Al sputtered layers on $Si_3N_4$ and Invar42 was effective in increasing the mechanical strength of these joints, more than 10 joints were prepared analyzed by FESEM, EDS and tested by SLO test (a sketch of these joined samples is in Figure 7A)

Figure 7B and C shows the FESEM results on polished cross section Al-sputtered $Si_3N_4$ and Invar42 joined by S-Bond: a thin interface layer formed between S-Bond and the Al sputtered layers on both $Si_3N_4$ and Invar42 is evident. As a comparison, the absence of such a reaction layer between S-Bond and $Si_3N_4$-to-Invar42 joints is clear in Figure 2B.

Figure 8A shows a typical result obtained after SLO test: the joining material is visible on both sides. A thorough examination of the fracture surfaces is shown in Figure 8B and C: SEM and EDS on both sides confirmed the presence of a Zn-Al rich layer at the interface after SLO test, which gave SLO shear strength compatible with reported in the S-Bond data sheet, 26 ± 7 MPa.

Table 1 summarizes all SLO results at room temperature and at 270°C (for Al sputtered Si3N4/Invar42): they are still lower values than those measured for S-Bond joined Al/Al, but in the same range. The difference in mechanical strength for joined samples without sputtered Al on both sides is striking.

## 3 | CONCLUSIONS

The joining of $Si_3N_4$ to Invar42 without surface modification resulted in very low lap shear strength (2.7 ± 1.2 MPa), much lower than that of $Si_3N_4$–$Si_3N_4$ (11 ± 4 MPa) and Al–Al (> 58 MPa) joints, indicating poor interfacial bonding. This study confirms that S-Bond does not establish a strong chemical bond with $Si_3N_4$ in the absence of surface activation. Sputtering with Cr or Zn offered no significant improvement, as no interfacial reaction layers formed at the soldering temperature (~450°C). In contrast, as suggested by the Al–Al joints' strength, Al sputtering promoted the formation of a reaction layer, raising the strength to 26 ± 7 MPa.

While sputtered Al enhanced bonding, it introduced additional process complexity and cost, and the resulting mechanical strength remained below what measured for the Al–Al joints, suggesting that an improvement in the Al layer on $Si_3N_4$ might be useful. The Al layer optimization might also mitigate the observed drop in strength at 270°C (14 ± 4 MPa), which might highlight concerns regarding thermal stability and long-term reliability under sustained or cyclic thermal loads.[34]

However, it must be underlined that this joining process is best suited for low-temperature applications (~300°C), aligning with the recommended service limit of S-Bond alloys (≤80%–90% of their solidus temperature).

Finally, achieving high mechanical performance in $Si_3N_4$–metal joints will require further process optimization.

## ACKNOWLEDGMENTS

Authors would like to thank Sergio Perero, Dario Alidoost and Giancarmine Muto, Politecnico di Torino, for their contribution to some parts of the experimental activity.

Open access publishing facilitated by Politecnico di Torino, as part of the Wiley - CRUI-CARE agreement.

## ORCID

*Stefano De La Pierre* https://orcid.org/0000-0003-3930-5234

## REFERENCES

1. Krstic Z, Krstic VD. Silicon nitride: the engineering material of the future. J Mater Sci. 2011;47(2):535–52. https://doi.org/10.1007/s10853-011-5942-5
2. Khod S, Goswami M. Simulation and empirical equation for thermal stress in $Al_2O_3/Si_3N_4$ ceramic joints brazed to Kovar/Monel metal alloys. Int J Appl Ceram Technol 2025;22:e15141. https://doi.org/10.1111/ijac.15141
3. Peteves SD, Ceccone G, Paulasto M, Stamos V, Yvon P. Joining silicon nitride to itself and to metals. J Miner Metals Mater Soc. 1996;48:48–52. https://doi.org/10.1007/BF03221363
4. Ceccone G, Nicholas MG, Peteves SD, Tomsia AP, Dalgleish BJ, Glaeser AM. An evaluation of the partial transient liquid phase bonding of Si3N4 using Au coated Ni22Cr foils. Acta Mater. 1996;44:657–67. https://doi.org/10.1016/1359-6454(95)00187-5
5. Kim JJ, Park JW, Eagar TW. Interfacial microstructure of partial transient liquid phase bonded $Si_3N_4$-to-inconel 718 joints. Mater Sci Eng A. 2003;344:240–44. https://doi.org/10.1016/S0921-5093(02)00402-1
6. Chen Z, Cao MS, Zhao QZ, Zou JS. Interfacial microstructure and strength of partial transient liquid-phase bonding of silicon nitride with Ti/Ni multi-interlayer. Mater Sci Eng A. 2004;380:394–401. https://doi.org/10.1016/j.msea.2004.04.012
7. Klemm H. Silicon nitride for high-temperature applications. J Am Ceram Soc. 2010;93:1501–22. https://doi.org/10.1111/j.1551-2916.2010.03839.x
8. Singh M, Asthana R, Varela FM, Martínez-Fernández J. Microstructural and mechanical evaluation of a Cu-based active braze alloy to join silicon nitride ceramics. J Eur Ceram Soc. 2011;31:1309–16. https://doi.org/10.1016/j.jeurceramsoc.2010.07.022
9. He Y, Zhang J, Lv P, Liu C. Characterization of the Si3N4/42CrMo joints vacuum brazed with Pd modified filler alloy for high temperature application. Vacuum. 2014;109:86–93. https://doi.org/10.1016/j.vacuum.2014.06.027
10. Lan L, Yu J, Yang Z, Li C, Ren Z, Wang Q. Interfacial microstructure and mechanical characterization of silicon nitride/nickel-base superalloy joints by partial transient liquid phase bonding. Ceram Int. 2016;42:1633–39. https://doi.org/10.1016/j.ceramint.2015.09.115
11. Lan L, Xuan W, Wang J, Li C, Ren Z, Yu J, et al. Interfacial microstructure of partial transient liquid phase bonding of $Si_3N_4$ to nickel-base superalloy using Ti/Au/Ni interlayers. Vacuum. 2016;130:105–8. https://doi.org/10.1016/j.vacuum.2016.04.033
12. Lan L, Ren Z, Yu J, Li C, Zhong Y. Interfacial microstructure and high-temperature strength in silicon nitride/nickel-based superalloy bonding. J Adhes Sci Technol. 2016;30:1430–40. https://doi.org/10.1080/01694243.2016.1146393
13. Morales-Pérez M, Ceja-Cárdenas L. Interfacial characterization in the brazing of silicon nitride to niobium joining using a double interlayer. Mater Charact. 2017;131:316–23. https://doi.org/10.1016/j.matchar.2017.07.026
14. Tunçkan O, Turan D, Doğan A, Turan S. Characterization of the interfaces formed at the silicon nitride superalloy joints. J Austr Ceram Soc. 2017;53:83–89.
15. Xu XP, Liu QM, Xia CZ, Zou JS. Microstructure and properties of $Si_3N_4$ ceramics and 304 stainless steel brazed joint with Cu/Ag-Cu/Ti laminated filler metal. High Temp Mater Process. 2018;37:597–602. https://doi.org/10.1515/htmp-2016-0183
16. Ong S, Tobe H, Sato E. Intermetallics evolution and fracture behavior of Nb interlayer inserted $Si_3N_4$/Ti joints brazed with AgCuTi filler. Mater Sci Eng A. 2019;762:138096. https://doi.org/10.1016/j.msea.2019.138096
17. Titanium Brazing. 2014. http://www.titanium-brazing.com/BrzngNwsltr_004.htm. Accessed February 27 2025.
18. Sun L, Wei Q, Fang J, Liu C, Zhang J. Brazing of porous $Si_3N_4$ ceramic to Invar alloy with a novel Cu–Ti filler alloy: microstructure and mechanical properties. Ceram Int. 2021;47(2):2068–76. https://doi.org/10.1016/j.ceramint.2020.09.039
19. NASA Technical Reports Server. 2019. https://ntrs.nasa.gov/search.jsp?R=20130013143. Accessed February 27, 2025.
20. Suganuma K, Miyamoto Y, Koizumi M. Joining of ceramics and metals. Annu Rev Mater Sci. 1988;18:47–73. https://doi.org/10.1146/annurev.ms.18.080188.000403
21. Wang T, Ivas T, Lee W, Leinenbach C, Zhang J. Relief of the residual stresses in $Si_3N_4$/Invar joints by multi-layered braze structure—experiments and simulation. Ceram Int. 2016;42:7080–87. https://doi.org/10.1016/j.ceramint.2016.01.096
22. Xu H, Wang J, Fan F, Zhang Z, Zhang D, Wu H, et al. Competitive correlation between the interface layers determines the shear strength in kovar/AgCuTi/$Si_3N_4$ joints. Int J Appl Ceram Technol 2024;22(2). https://doi.org/10.1111/ijac.14920
23. Shirzadi AA, Zhu Y, Bhadeshia H. Joining ceramics to metals using metallic foam. Mater Sci Eng A. 2008;496:501–6. https://doi.org/10.1016/j.msea.2008.06.007
24. Guo W, Zhang H, Ma K, Zhu Y, Zhang H, Qi B, et al. Reactive brazing of silicon nitride to Invar alloy using Ni foam and

AgCuTi intermediate layers. Ceram Int. 2019;45(11):13979–87. https://doi.org/10.1016/j.ceramint.2019.04.097
25. Selverian JH, Kang S. Ceramic-to-metal joints. II: Performance and strength prediction. Ceram Bull. 1992;71(10):1511–20.
26. Zhou Y, Bao FH, Ren JL, North TH. Interlayer selection and thermal stresses in brazed $Si_3N_4$− steel joints. Weld J. 2013;7:863–68.
27. Ong FS, Tobe H, Fujii G, Sato E. Microstructural evolution and mechanical characterization of Nb-interlayer-inserted Ti–6Al–4 V/$Si_3N_4$ joints brazed with AuNiTi filler. Mater Sci Eng A. 2020;778:139093. https://doi.org/10.1016/j.msea.2020.139093
28. Rajendran SH, Lee GA, Park JY, Kang YS, Jung JP. Joining $Si_3N_4$ ceramic to Invar using Mo mesh and Cu foil interlayer. Materi Chem Phys. 2024;313:128732. https://doi.org/10.1016/j.matchemphys.2023.128732
29. Zhao T, Mo D, Li X, Gong H. Interfacial microstructure and mechanical properties of $Si_3N_4$/invar joints using Ag–Cu–In–Ti with Cu foil as an interlayer. Materials Testing. 2024;66(2):207–14. https://doi.org/10.1515/mt-2023-0221
30. Salvo M, Casalegno V, Suess M, Gozzelino L, Wilhelmi C. Laser surface nanostructuring for reliable $Si_3N_4$/$Si_3N_4$ and $Si_3N_4$/invar joined components. Ceram Int. 2018;44(11):12081–87. https://doi.org/10.1016/j.ceramint.2018.03.226
31. Koleňák, Provazník M, Igor S. *Soldering by the Active Lead-Free Tin and Bismuth-based Solders*. IntechOpen; 2018. https://doi.org/10.5772/intechopen.81169
32. S-Bond Technologies Blog. 2011. https://s-bond.com/blog/sapphire-window-sealing-with-s-bond/ Accessed February 27, 2025
33. US Patent US20150099619A1.
34. Ngo MC, Miyazaki H, Hirao K, Fukushima M. Analysis of thermal strain of metallized silicon nitride substrate under cyclic thermal loading by digital image correlation. Int J Appl Ceram Technol 2024;1032–41. https://doi.org/10.1111/ijac.14565

**How to cite this article:** De La Pierre S, Benelli A, Ferraris M, Di Martino D, Vivenzio F, Napolitano R. Soldering Si3N4 to Invar42 by a localized heating process. Int J Appl Ceram Technol. 2026;23:e70118. https://doi.org/10.1111/ijac.70118